Journal of Quantitative Spectroscopy & Radiative Transfer 122 (2013) 25–30

Contents lists available at SciVerse ScienceDirect

Journal of Quantitative Spectroscopy & Radiative Transfer

journal homepage: www.elsevier.com/locate/jqsrt

Black and brown carbon fractal aggregates from combustion of two fuels widely used in Asian rituals

Rajan K. Chakrabarty [a,b,*], Ian J. Arnold [a], Dianna M. Francisco [b], Benjamin Hatchett [b], Farnaz Hosseinpour [b], Marcela Loria [b], Ashok Pokharel [b], Brian M. Woody [b]

[a] Laboratory for Aerosol Science, Spectroscopy, and Optics, Division of Atmospheric Sciences, Desert Research Institute, Reno, NV 89512, USA
[b] Graduate Program in Atmospheric Sciences, University of Nevada, Reno, NV 89557, USA

ARTICLE INFO

Article history:
Received 7 August 2012
Received in revised form
14 December 2012
Accepted 17 December 2012
Available online 28 December 2012

Keywords:
Combustion aerosols
Asia
Brown carbon
Black carbon
Fractal aggregates

ABSTRACT

Incense sticks and mustard oil are the two most popular combustion fuels during rituals and social ceremonies in Asian countries. Given their widespread use in both closed and open burning activities, it is important to quantify the spectral radiative properties of aerosols emitted from the combustion of both fuels. This information is needed by climate models to assess the impact of these aerosols on radiative forcing. In this study, we used a 3-wavelength integrated photoacoustic-nephelometer – operating simultaneously at 405, 532 and 781 nm – to measure the optical coefficients of aerosols emitted from the laboratory combustion of mustard oil lamp and two types of incense sticks. From the measured optical coefficients at three wavelengths, time-varying single scattering albedo (SSA), absorption Ångström exponent (AAE), and scattering Ångström exponent (SAE) were calculated. For incense smoke particles, the time-averaged mean AAE values were found to be as high as 8.32 (between 405 and 532 nm) and 6.48 (between 532 and 781 nm). This spectrally-varying characteristic of AAE indicates that brown carbon – a class of organic carbon which strongly absorbs solar radiation in the blue and near ultraviolet – is the primary component of incense smoke aerosols. For aerosols emitted from the burning of mustard oil lamp, the time-averaged mean AAE values were ~1.3 (between 405 and 781 nm) indicating that black carbon (BC) is the primary constituent. Scanning electron microscopy combined with image processing revealed the morphology of incense smoke aerosols to be non-coalescing and weakly-bound aggregates with a mean two-dimensional (2-d) fractal dimension (D_f)=1.9 ± 0.07, while the mustard oil smoke aerosols had typical fractal-like BC aggregate morphology with a mean 2-d D_f=1.85 ± 0.09.

1. Introduction

Burning of incense sticks and mustard oil lamps is a common sight in most Asian countries. Both fuels find wide use in a range of activities, from daily recreational burning in homes to large-scale burning in semi-open and open sites such as temples and religious ceremonies [1,2]. In India, mustard oil lamps are lit in homes, porches, and temples for prolonged hours on a daily basis, while in other Asian countries, incense burning is the more prevalent ritual. Fig. 1 shows a typical scene of burning of incense sticks and oil lamps outside an Indian temple. Since burning of both fuels is customary in Asian cultures, their resulting emissions and consequences on the environment and health are often overlooked with few scientific studies only conducted so far. A recent study [3] has identified emissions from rituals and religious ceremonies

* Corresponding author at: Laboratory for Aerosol Science, Spectroscopy, and Optics, Division of Atmospheric Sciences, Desert Research Institute, Reno, NV 89512, USA. Tel.: +1 775 674 7003.
E-mail address: rajan.chakrabarty@dri.edu (R.K. Chakrabarty).

0022-4073/$ - see front matter © 2012 Elsevier Ltd. All rights reserved.
http://dx.doi.org/10.1016/j.jqsrt.2012.12.011

Fig. 1. A typical scene from outside a temple in India—large-scale burning of incense sticks and oil lamps.

to contribute significant amounts of black carbon (BC; ~73 Gigagrams/year) and organic carbon (~102 Gigagrams/year) to the total carbonaceous aerosol emissions from India. From a climate standpoint, emissions of carbonaceous aerosols from Asian countries represent one of the largest uncertainties in estimation of aerosol radiative forcing by climate models [4,5]. To reduce this large uncertainty, studies are needed to improve our understanding and parameterization of region-specific combustion-generated aerosols [6].

Jetter et al. [7] were one of the first to characterize the emissions from 23 different types of incense sticks. In their experiments, fine particulate matter $PM_{2.5}$ (aerosols less than 2.5 micrometers (μm) in diameter) emission rates ranged from 7 to 202 mg h^{-1}, and $PM_{2.5}$ emission factors ranged from 5 to 56 mg g^{-1} of incense burned. They concluded that $PM_{2.5}$ constitute the majority of emissions from incense burning. Wang et al. [8] measured the aerosol concentrations emitted from incense burning in two temples in Hong Kong, and found that majority aerosols emitted were carbonaceous in nature with $PM_{2.5}$ constituting 82% of total aerosol mass. Ji et al. [9] measured the aerosol number size distribution from incense smoke to be less that 1 μm in diameter, and the particle mass median aerodynamic diameter ranging from 150 to 300 nm. Yang et al. [10] reported elevated concentrations of toxic poly-cyclic aromatic hydrocarbons (PAHs) in incense smoke, implying that the incense smoke could have a high potential health effects. Studies on the radiative properties of aerosols emitted from ritual fuels are limited at best. Gyawali et al. [11] recently reported observation of enhanced absorption in the near-UV (ultraviolet) wavelength by carbonaceous aerosols emitted from incense burning. This study is inspired by their preliminary findings, and is intended to provide a more detailed picture of the multi-spectral optical properties of emissions from commonly used Asian ritual fuels.

Emission of carbonaceous aerosols in the atmosphere influences the earth's radiation balance and climate and the health of living beings on scales ranging from local to global [12,13]. Carbonaceous aerosols are emitted from both high and low temperature combustion systems, and directly alter the global short-wave radiation budget by absorbing and scattering light [14]. Their interaction with solar radiation reduces the net shortwave radiative flux to the earth's surface. It is now well-known that high-temperature combustion processes emit BC fractal-like aggregates – made up of repeating small spherical (monomer) particles – which is a significant light absorber in the shortwave solar spectra [14]. Low-temperature combustion emits a class of light-absorbing organic carbon compounds – brown carbon (BrC) – that has only been recently shown to strongly absorb solar radiation in the blue and near-UV [14,15], thereby modifying radiative forcing [16] and actinic fluxes [17]. Light absorption by both BC and BrC aerosols is significant and results in warming of the atmosphere in the vicinity of the aerosols [14,18,19], potentially affecting atmospheric stability and changing precipitation patterns [19–21].

In this paper, we report our measurements of the radiative and physical properties of aerosol emissions from burning of incense stick and mustard oil lamps. The smoke particles were characterized using a suite of instruments, namely a scanning electron microscopy (SEM), a 3-wave length integrated photoacoustic-nephelometer (IPN), and a scanning mobility particle sizer (SMPS). The SEM combined with image analysis was used to provide direct observation of the particle morphology and elemental composition of the particles. The IPN provided real-time measurements of scattering and absorption coefficients in three wavelengths—405, 532 and 781 nanometers (nm). Spectrally and time-varying measurements of the optical coefficients were used to calculate particle Absorption Ångström Exponent (AAE), Scattering Ångström Exponent (SAE), and Single Scattering Albedo (SSA)—optical parameters necessary for calculation of radiative forcing by aerosols in climate models [19]. The SMPS yielded measurements of particle number size distributions. SEM images of aerosol aggregates were analyzed for their fractal dimensions (D_f) in two dimensions (2-d). Section 2 of this paper describes the experimental techniques and analytical methods used in this study. Measurement and analysis results of the optical and physical properties of aerosols are presented in Section 3.

2. Experimental and analytical techniques

Experiments were conducted at the Carter Family Optics facility of the Desert Research Institute as part of an advanced graduate-level course titled "*ATMS 743: Cloud and Aerosol Physics*" offered at the University of Nevada, Reno during Spring 2012. Two popular types of Asian incense sticks – Incense 1 (Mogra fragrance) and Incense 2 (Amber fragrance) – and cotton wick soaked in pure mustard seed oil (manufactured by Dabur India Inc.) in a clay cup were lit individually in a fume-hood. The burning of an incense stick, on an average, lasted for ~17 min, and sampling of aerosols was done for the entire time period. Sampling of aerosols from mustard oil lamp burning was done for 5 min. For each fuel type, two runs of experiments were conducted to ensure repeatability and reliability of the measurements. The incense sticks used in this study were manufactured in India, and their material

composition included herbal and wood powder, fragrance material and adhesive powder. Smoke particles from the fume-hood were transported in parallel to a 3-wavelegnth IPN and a SMPS using conductive tubing, which helped to minimize particle losses during transport [22].

The 3-wavelength IPN (Model PASS-3, Droplet Measurement Technologies, Inc., Boulder, CO) used in this study consists of 405, 532, and 781 nm diode lasers and a reciprocal integrating nephelometer aligned in an acoustic resonator. The instrument measures particle light absorption using the photoacoustic effect—the laser beam induces particle temperature changes and subsequent pressure changes of the surrounding air at the modulation frequency [23]. The reciprocal integrating nephelometer adds a cosine-weighted optical detector to the instrument that measures the integrated (over $\sim 4\pi$) scattering from the sample volume yielding the scattering coefficient (β_{sca}) [24]. The instrument simultaneously measures β_{sca} and absorption (β_{abs}) coefficients at the three wavelengths allowing calculation of the spectrally-varying optical parameters—SSA, AAE and SAE.

SSA is the ratio of scattering to extinction coefficients, with the extinction coefficients ($\beta_{sca}/(\beta_{abs}+\beta_{sca})$) [25]. Ångström coefficients are commonly used to parameterize the slow wavelength dependence of aerosol scattering, absorption, and extinction coefficients. AAE is defined for a pair of wavelengths λ_1 and λ_2 as the exponent in a power law expressing the ratio of the absorption coefficients β_{abs} (λ_1,λ_2) as follows [26]:

$$AAE(\lambda_1\lambda_2) = \frac{\ln[\beta_{abs}(\lambda_1)/\beta_{abs}(\lambda_2)]}{\ln[\lambda_2/\lambda_1]} \quad (1)$$

AAE is an optical descriptor of the inherent material property. For BC particles, typical values of AAE ≈ 1, while for pure BrC particles AAE > 4 [14,18]. SAE is defined similarly to AAE in Eq. (1), with β_{sca} (λ_1,λ_2) taking the place of β_{abs} (λ_1,λ_2).

For SEM analysis, particles were impacted thermophoretically from the over-fire region of the burns onto double-sided conductive tapes stuck onto SEM metal stubs [27]. The metal stubs were hand-held and exposed for a few seconds to avoid particle overloading. After exposure, the stubs were stored in a refrigeration unit to avoid any transformation of the particles due to aging. A 1 nm thick layer of platinum coating was applied to the conductive tapes prior to SEM analysis in order to inhibit charging of aerosol particles during the analysis. A Hitachi Scanning Electron Microscope (Model S-4700), maintained by the University of Nevada, Reno's Department of Materials Science and Engineering, was used to analyze the coated samples.

Combustion aerosols often have complex aggregate morphologies [28]. Over the past three decades, fractal mathematics has been used successfully to characterize their non-spherical morphologies [29]. Of all the available fractal characterization techniques, the *box-counting* technique has found extensive use in the area of aerosol science [30]. Calculating the 2-d D_f using the box-counting technique involves drawing boundaries of squares of increasing size upon a 2-d, pixilated image of a fractal aggregate centered on the aggregate center of mass. For every boundary, the number of pixels occupied by the particle is counted. The 2-d D_f is then calculated as the linear regression slope of the linear portion of the log-log curve generated by plotting boundary size against pixel count. For this study, eleven representative images corresponding to each fuel type were selected for morphology and shape quantification.

The SMPS instrument consists of a scanning Differential Mobility Analyzer (DMA; Model 3080, TSI, St. Paul, MN) and a Condensation Particle Counter (CPC; Model 3010, TSI, St. Paul, MN) in series, and measures the particle number size distribution in terms of the mobility diameter for particles below 800 nm. The DMA scans through the particle distribution by stepping through 39 voltage differences over 2–10 min, while the CPC counts the number of particles in each size bin. In this study, the scanning DMA was operated with a sheath/aerosol flow ratio of 10:1 (sheath flow=3 L/min; aerosol flow=0.3 L/min), yielding a DMA size transmission width of approximately $\pm$10%.

3. Results and discussion

Fig. 2 shows the wavelength-dependent AAEs of aerosols emitted from the two fuel types as function of time. The plots are from first of the two sets of experiments conducted. The second set of experiments gave similar measurements with very little (1–2%) variability. High values of AAE (>4) for both incense types (Fig. 2b and c)

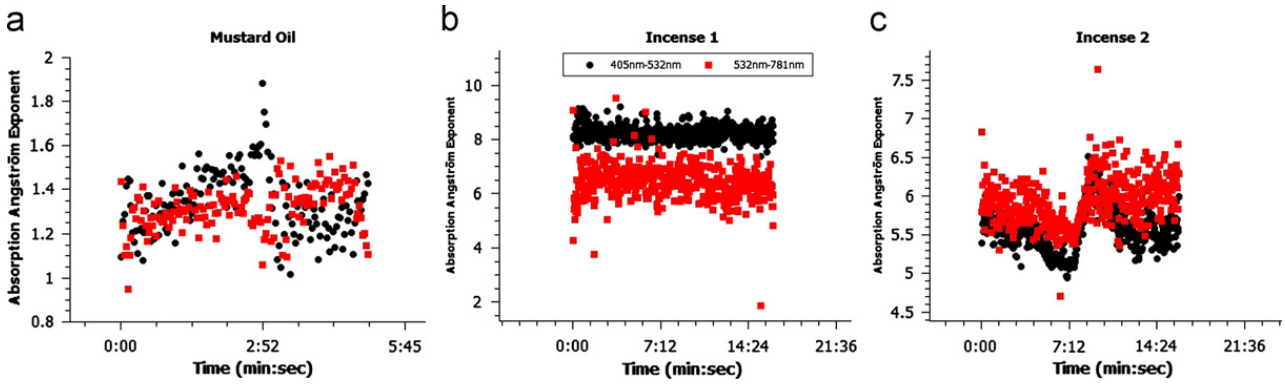

Fig. 2. Ångström Absorption exponents calculated between 405 and 532 nm and between 532 and 781 nm as a function of time for aerosols emitted from laboratory combustion of (a) mustard oil lamp, (b) incense stick type 1 (Mogra fragrance) and (c) incense stick type 2 (Amber fragrance).

indicate that BrC is the dominant and primary component of the emitted aerosols. For incense 1, the time-averaged mean AAEs were 8.32 (between wavelengths 405 and 532 nm) and 6.48 (between 532 and 781 nm). For incense 2, the time-averaged mean AAE values were a bit lower in comparison to incense 1– 5.65 (between 405 and 532 nm) and 5.94 (between 532–781 nm). In contrast, the dominant material in emissions from mustard oil burning is BC with mean AAE values remaining wavelength-dependent at ~1.32 (between 405 and 781 nm).

SEM images of particles from mustard oil burning (Fig. 3A) reveal chain-like fractal aggregate morphology typical of BC aerosols. This observation is in conformity with aerosol morphology predicted from high-temperature combustion systems, which are dominated by Brownian motion dynamics [14]. On the other hand, incense stick burning is a moderate-to-low temperature "smoldering" combustion process, and the morphology of emitted particles showed up as non-coalescing but weakly-bound aggregates (Fig. 3B). This morphology is distinct from BC fractal aggregates in that BC aggregates are made of coalescing spherical monomers, strongly-bound, and does not decompose when exposed to electron beams. In this study, the incense aggregates tended to melt and decompose when viewed under the SEM, indicating the presence of strong organic coatings [31]. The box counting procedure for calculating the aggregate 2-d D_f yielded a mean $D_f = 1.85 \pm 0.09$ for mustard oil aggregates and a mean $D_f = 1.9 \pm 0.07$ for incense aggregates. It is to be noted that there might exist significant uncertainties in the calculated 2-d D_f values using the box counting procedure as pointed out recently by Chakrabarty et al. [30].

For incense aggregates, the median monomer diameter was 32.5 ± 0.8 nm and their median aggregate mobility diameter was 182.4 ± 17.8 nm. For mustard oil aggregates, the median monomer diameter was 31.8 ± 5.2 nm and their median aggregate mobility diameter was 296.8 ± 73.9 nm. The aggregate size ranges measured for both fuel types in this study are in conformity with past size measurements of BC and incense aerosols [9,28].

Figs. 4 and 5 show the wavelength-varying SSAs and SAEs of the two aerosol types as function of time. For mustard oil aerosols, the mean value of SSA is 0.4 (Fig. 4a), which is typical for BC aerosols [32]. BC aerosols dominate light absorption in the shortwave, reflecting their low values of SSA. During our experiments, the mustard oil flame often underwent flickering which resulted in fluctuating SSAs. Flickering affects the combustion conditions, which in turn affects the amount of organic carbon released from a flame [33]. Increase in emission of organic materials results in increased SSA, which explains the intermittent increase in SSA of BC aerosols in Fig. 4a. For

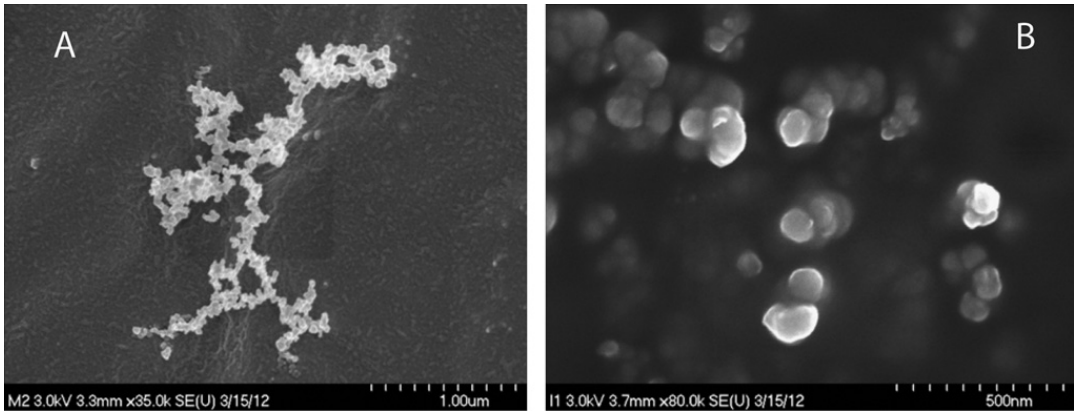

Fig. 3. (A) A typical fractal-like black carbon aggregate formed by the high-temperature combustion of mustard seed oil lamp. The greater thermal kinetic energy promotes aggregation via Brownian motion; (B) non-coalescing and weakly-bound brown carbon aggregates generated in the low-temperature combustion of incense sticks.

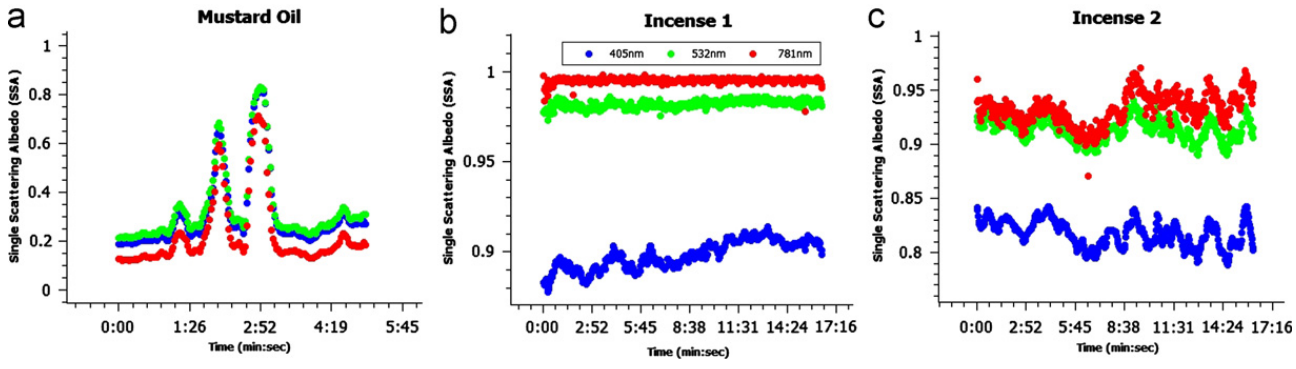

Fig. 4. Single scattering albedo calculated at 405, 532 and 781 nm as function of time for aerosols emitted from laboratory combustion of (a) mustard oil lamp, (b) incense stick type 1, and (c) incense stick type 2.

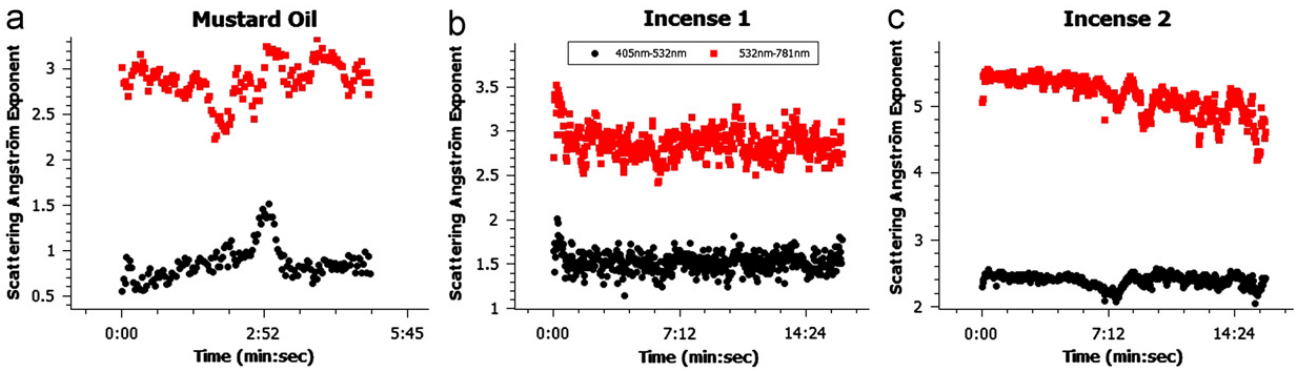

Fig. 5. Scattering Ångström exponents calculated between 405 and 532 nm and between 532 and 781 nm as function of time for aerosols emitted from laboratory combustion of (a) mustard oil lamp, (b) incense stick type 1, and (c) incense stick type 2.

incense smoke aerosols (Fig. 4b and c), their increasing SSA in the 405–781 nm is associated with their rapidly falling values of AAEs (see Fig. 2b and c). Their time-averaged mean SSA values ~1 in the 532–781 nm wavelength range agrees with SSA values observed for BrC aerosols emitted from combustion of wildland fuels [18].

The time-averaged mean values of SAE for BC aerosols from mustard oil burning were 0.8 (between wavelengths 405 and 532 nm) and 2.9 (between 532 and 781 nm) (Fig. 5a). For both incense types (Fig. 5b and c), the ranges of SAE values were between 1.5 and 2.5 (405–532 nm) and between 2.8 and 5 (532–781 nm). Unlike AAE, the wavelength dependence of the scattering coefficients of carbonaceous aerosols may not be the best way to characterize their material property. Instead, the SSA Ångström Exponent (SSAAE) may be a better indicator of the different carbonaceous aerosol types. Calculated SSAAE values for BrC aerosols emitted from incense smoke in this study were negative. It has been recently shown that negative SSAAEs are a useful criteria for identifying BrC aerosols [18].

4. Summary

The radiative properties (in wavelength range 405–781 nm) and microstructure of aerosols emitted from the combustion of two widely used Asian ritual fuels – incense and mustard oil – have been studied. For particles from incense combustion, their strong spectrally-varying optical characteristics indicate that brown carbon – a class of organic carbon which strongly absorbs solar radiation in the blue and near ultraviolet – is the primary component in them. SEM combined with image processing showed that these brown carbon aerosols had non-coalescing and weakly-bound aggregate morphology. Aerosols emitted from the burning of mustard oil lamp had black carbon as the primary constituent, and typical fractal-like BC aggregate morphology. Given the widespread use of incense sticks in semi-open and open activities all over Asia, the brown carbon aerosols emitted by their burning may have significant implications for radiative forcing in the near-UV and UV wavelengths causing enhanced atmospheric absorption and warming.

Acknowledgment

This material is based upon work supported by the DRI VPAA Course Development Funds, by the DRI DAS Faculty Support Funds, by the NASA EPSCoR under Cooperative Agreement no. NNX10AR89A, and by NASA ROSES under Grant NNX11AB79G. We acknowledge Dr. Johann Engelbrecht for loaning his 3-wavelength IPN to conduct this study, and Dr. Hans Moosmüller for his valuable discussions on data analysis and interpretation.

References

[1] Estrellan CR, Iino F. Toxic emissions from open burning. Chemosphere 2010;80:193–207.
[2] Navasumrit P, Arayasiri M, Hiang OMT, Leechawengwongs M, Promvijit J, Choonvisase S, et al. Potential health effects of exposure to carcinogenic compounds in incense smoke in temple workers. Chem Biol Interact 2008;173:19–31.
[3] Pervez S, Dewangan S, Chakrabarty RK, Pervez Y. Significant contribution of emissions from asian religious and cultural activities to atmospheric brown clouds. In: Proceedings of the visibility and atmospheric optics conference. Whitefish, Montana, USA: Air and Waste Management Association; 2012.
[4] Gustafsson O, Krusa M, Zencak Z, Sheesley RJ, Granat L, Engstrom E, et al. Brown clouds over South Asia: biomass or fossil fuel combustion? Science 2009;323:495–8.
[5] Ramanathan V, Ramana M. Atmospheric brown clouds: long-range transport and climate impacts. Em-Pittsburgh-Air and Waste Management Association; 2003. p. 28–33.
[6] Solomon S. Climate change 2007: the physical science basis: contribution of Working Group I to the Fourth Assessment Report of the Intergovernmental Panel on Climate Change. Cambridge University Press, Cambridge, United Kingdom and New York, NY, USA; 2007.
[7] Jetter JJ, Guo Z, McBrian JA, Flynn MR. Characterization of emissions from burning incense. Sci Total Environ 2002;295:51–67.
[8] Wang B, Lee S, Ho K, Kang Y. Characteristics of emissions of air pollutants from burning of incense in temples, Hong Kong. Sci Total Envir 2007;377:52–60.
[9] Ji X, Le Bihan O, Ramalho O, Mandin C, D'Anna B, Martinon L, et al. Characterization of particles emitted by incense burning in an experimental house. Indoor Air 2010;20:147–58.
[10] Yang CR, Lin TC, Chang FH. Particle size distribution and PAH concentrations of incense smoke in a combustion chamber. Environ Pollut 2007;145:606–15.
[11] Gyawali M, Arnott W, Zaveri R, Song C, Moosmüller H, Liu L, et al. Photoacoustic optical properties at UV, VIS, and near IR wavelengths for laboratory generated and winter time ambient urban aerosols. Atmos Chem Phys 2012;12:2587–601.
[12] Haywood J, Ramaswamy V. Global sensitivity studies of the direct radiative forcing due to anthropogenic sulfate and black carbon aerosols. J Geophys Res 1998;103:6043–58.
[13] Vedal S. Ambient particles and health: lines that divide. J Air Waste Manage Assoc 1997;47:551–81.

[14] Moosmuller H, Chakrabarty RK, Arnott WP. Aerosol light absorption and its measurement: a review. J Quant Spectrosc Radiat Transfer 2009;110:844–78.
[15] Andreae MO, Gelencsér A. Black carbon or brown carbon? The nature of light-absorbing carbonaceous aerosols Atmos Chem Phys 2006;6:3131–48.
[16] Solomon S, Qin D, Manning M, Chen Z, Marquis M, Averyt KB, et al. Climate change 2007: the physical science basis. Contribution of Working Group I to the Fourth Assessment report of the Intergovernmental Panel on Climate Change. Geneva, Switzerland: IPCC Secretariat; 2007.
[17] Jacobson MZ. Studying the effects of aerosols on vertical photolysis rate coefficient and temperature profiles over an urban airshed. J Geophys Res 1998;103:10593–604.
[18] Chakrabarty R, Moosmüller H, Chen L, Lewis K, Arnott W, Mazzoleni C, et al. Brown carbon in tar balls from smoldering biomass combustion. Atmos Chem Phys 2010;10:6363–70.
[19] Chakrabarty RK, Garro MA, Wilcox EM, Moosmüller H. Strong radiative heating due to wintertime black carbon aerosols in the Brahmaputra River Valley. Geophys Res Lett 2012;39:L09804.
[20] Meehl GA, Arblaster JM, Collins WD. Effects of black carbon aerosols on the Indian monsoon. J Clim 2008;21:2869–82.
[21] Wang C. Impact of direct radiative forcing of black carbon aerosols on tropical convective precipitation. Geophys Res Lett 2007:34.
[22] Chakrabarty RK, Moosmuller H, Arnott WP, Garro MA, Slowik JG, Cross ES, et al. Light scattering and absorption by fractal-like carbonaceous chain aggregates: comparison of theories and experiment. Appl Opt 2007;46:6990–7006.
[23] Arnott WP, Moosmüller H, Rogers CF, Jin T, Bruch R. Photoacoustic spectrometer for measuring light absorption by aerosol: instrument description. Atmos Environ 1999;33:2845–52.
[24] Abu-Rahmah A, Arnott WP, Moosmüller H. Integrating nephelometer with a low truncation angle and an extended calibration scheme. Meas Sci Technol 2006;17:1723–32.
[25] Bohren CF, Huffman DR. Absorption and scattering of light by small particles. New York: J. Wiley & Sons; 1983.
[26] Moosmüller H, Chakrabarty R, Ehlers K, Arnott W. Absorption Ångström coefficient, brown carbon, and aerosols: basic concepts, bulk matter, and spherical particles. Atmos Chem Phys 2011;11:1217–25.
[27] Dobbins RA, Megaridis CM. Morphology of flame-generated soot as determined by thermophoretic sampling. Langmuir 1987;3:254–9.
[28] Chakrabarty RK, Moosmüller H, Garro MA, Arnott WP, Walker J, Susott RA, et al. Emissions from the laboratory combustion of wildland fuels: particle morphology and size. J Geophys Res 2006;111:D07204.
[29] Sorensen CM. Light scattering by fractal aggregates: a review. Aerosol Sci Technol 2001;35:648–87.
[30] Chakrabarty RK, Garro MA, Garro BA, Chancellor S, Moosmüller H, Herald CM. Simulation of aggregates with point-contacting monomers in the cluster–dilute regime. Part 1: Determining the most reliable technique for obtaining three-dimensional fractal dimension from two-dimensional images. Aerosol Sci Technol 2010;45:75–80.
[31] Chakrabarty RK, Moosmüller H, Arnott WP, Garro MA, Walker J. Structural and fractal properties of particles emitted from spark ignition engines. Environ Sci Technol 2006;40:6647–54.
[32] Lewis K, Arnott WP, Moosmüller H, Wold CE. Strong spectral variation of biomass smoke light absorption and single scattering albedo observed with a novel dual-wavelength photoacoustic instrument. J Geophys Res 2008;113:D16203.
[33] Slowik JG, Cross ES, Han JH, Davidovits P, Onasch TB, Jayne JT, et al. An inter-comparison of instruments measuring black carbon content of soot particles. Aerosol Sci Technol 2007;41:295–314.